

This article was downloaded by:

On: 25 January 2011

Access details: *Access Details: Free Access*

Publisher *Taylor & Francis*

Informa Ltd Registered in England and Wales Registered Number: 1072954 Registered office: Mortimer House, 37-41 Mortimer Street, London W1T 3JH, UK



Journal of Macromolecular Science, Part A

Publication details, including instructions for authors and subscription information:

<http://www.informaworld.com/smpp/title~content=t713597274>

Free-Radical Copolymerization of Methyl Methacrylate and α -Methacrylophenone. II. Sequence Distribution through ^{13}C - ^1H NMR Spectroscopy

R. Roussel^a; J. C. Galin^a

^a Centre de Recherches sur les Macromolécules C.N.R.S., Strasbourg Cedex, France

To cite this Article Roussel, R. and Galin, J. C.(1977) 'Free-Radical Copolymerization of Methyl Methacrylate and α -Methacrylophenone. II. Sequence Distribution through ^{13}C - ^1H NMR Spectroscopy', *Journal of Macromolecular Science, Part A*, 11: 2, 347 – 377

To link to this Article: DOI: 10.1080/00222337708061273

URL: <http://dx.doi.org/10.1080/00222337708061273>

PLEASE SCROLL DOWN FOR ARTICLE

Full terms and conditions of use: <http://www.informaworld.com/terms-and-conditions-of-access.pdf>

This article may be used for research, teaching and private study purposes. Any substantial or systematic reproduction, re-distribution, re-selling, loan or sub-licensing, systematic supply or distribution in any form to anyone is expressly forbidden.

The publisher does not give any warranty express or implied or make any representation that the contents will be complete or accurate or up to date. The accuracy of any instructions, formulae and drug doses should be independently verified with primary sources. The publisher shall not be liable for any loss, actions, claims, proceedings, demand or costs or damages whatsoever or howsoever caused arising directly or indirectly in connection with or arising out of the use of this material.

Free-Radical Copolymerization of Methyl Methacrylate and α -Methacrylophenone. II. Sequence Distribution through ^{13}C -[^1H] NMR Spectroscopy

R. ROUSSEL and J. C. GALIN

Centre de Recherches sur les Macromolécules
C.N.R.S.
67083 Strasbourg Cedex, France

ABSTRACT

Sequence distribution in methyl methacrylate (A)-methacrylophenone (B) copolymers obtained by free-radical copolymerization at 60°C has been studied by ^{13}C -[^1H] NMR spectroscopy. Quantitative analysis of the resonance patterns of the quaternary carbon atom of A units and of the α - CH_3 carbon atoms of A and B units has been carried out, considering both compositional and configurational effects. All the kinetic and structural data may be readily taken into account by a scheme in which copolymerization obeys a penultimate unit model characterized by the four reactivity ratios $r_{AA} = 1.77 \pm 0.02$, $r_{BA} = 2.30 \pm 0.10$, $r_{BB} = 0.058 \pm 0.01$, $r_{AB} = 0.325 \pm 0.03$. The stereochemistry of the cross-propagation steps may be described by a single cotacticity parameter: $\sigma_{AB} = \sigma_{BA} \simeq 0.40$. Its relatively high value probably arises from the great steric hindrance and the high polarizability of the aromatic keto group of methacrylophenone.

INTRODUCTION

In the previous communication [1] we investigated the free-radical copolymerization of methyl methacrylate (MMA, monomer A) and methacrylophenone [$\text{CH}_2=\text{C}(\text{CH}_3)-\text{C}_6\text{H}_5$, MAP, monomer B] initiated at 60°C by azobisisobutyronitrile, either in bulk or in solution. The copolymerization is characterized by the competitive Diels-Alder condensation of MAP [2] and by very slow propagation and very high termination constants for MAP-terminated macroradicals. In the whole range of monomer feed composition ($0.05 \leq F_A \leq 0.95$), the reaction may be accounted for by a classical terminal unit model and the two reactivity ratios, $r_A = 1.77 \pm 0.02$ and $r_B = 0.110 \pm 0.006$. Nevertheless, because of the inability of MAP to undergo free-radical homopolymerization, we have suggested two more sophisticated processes: copolymerization with depropagation of MAP terminated growing chains, or copolymerization with penultimate effects on both monomers. The excellent agreement we observed previously between experimental compositional data and calculated curves [1] is not sufficient to ascertain a physical basis for these models.

In order to get a more accurate insight in the copolymerization mechanism we have focused our attention on the microstructure of the MMA-MAP copolymers. The present communication mainly deals with the analysis of sequence distribution by ^{13}C - ^1H NMR spectroscopy.

EXPERIMENTAL

MMA-MAP Copolymers, PMAP and PMMA Homopolymers

The MMA-MAP copolymer samples were obtained, as previously described, by free-radical copolymerization stopped at low conversion. The number of the sample refers to the run number indicated on Tables 2 and 3 of the preceding communication [1]. PMAP and PMMA (Röhm-Haas) are, respectively, an anionic [1] and a free-radical sample.

NMR Spectroscopy

The ^1H -NMR spectra were obtained at 100 MHz (Varian HA-100) or at 250 MHz (Cameca 250) on solutions of about 15% (w/v) in CDCl_3 , pyridine- d_6 , and *o*-dichlorobenzene.

The natural abundance ^{13}C -[^1H] NMR spectra were obtained on a Varian XL-100 spectrometer at 25.14 MHz by use of 15-30% (w/v) polymer solutions in CDCl_3 . Experimental conditions were the following: temperature, 32° C; pulse width, 60 μsec ; pulse delay, 0.6-2.0 sec; acquisition time, 0.6-0.8 sec; K-transients 3,000-50,000. These conditions have not been optimized. For the $\alpha\text{-CH}_3$ resonance the complex NMR patterns were simulated on a Du Pont -310 curve resolver, assuming Lorentzian shape for the different resonance peaks. Complications from variations in nuclear Overhauser enhancements were considered safely ignored for carbon atoms differing only in the steric configuration of neighboring units [3].

All the chemical shifts are expressed in ppm downfield from tetramethylsilane (TMS) used as reference.

RESULTS AND DISCUSSION

Berger and Kuntz [4] have pointed out that the copolymer microstructures are more sensitive to the copolymerization process than their overall compositions, and that the analysis of sequence distribution may allow to choose between different propagation mechanisms. Some experimental studies may be quoted as a good illustration of such an approach: penultimate effects for vinylidene chloride-isobutene [5, 6] or acrylonitrile-methyl methacrylate [7] systems; depropagation effects for methyl methacrylate-acrylonitrile [8] or α -methylstyrene-methyl methacrylate systems [9]. The same methodology may be obviously of great interest in the case of MMA-MAP copolymerization.

Influence of Depropagation and Penultimate Effects in Copolymerization on the Microstructure of MMA-MAP Copolymers

By using the experimental values of the reactivity ratios previously measured [1] and the statistical calculations described in Appendix I, we have determined different characteristic distribution parameters of the copolymers, assuming that copolymerization obeys one of the three following schemes: terminal unit model ($r_A = 1.775$, $r_B = 0.110$); copolymerization with simultaneous depropagation of the macroradicals $\sim\sim\text{BBB}\cdot$ ($r_A = 1.81$, $r_B = 0.174$, propagation-depropagation equilibrium constant $K = 0.12$); and penultimate unit model ($r_{AA} = 1.77$, $r_{BA} = 2.30$, $r_{BB} = 0.058$, $r_{AB} = 0.325$).

The average length of MMA and MAP blocks does not show a great sensitivity towards the copolymerization process, but appreciable differences clearly appear in the weight distribution of the MMA and MAP units measured by the weight fraction of a given monomer included in block of length n : $F_W(A_n)$ and $F_W(B_n)$; and the weight fraction of a given monomer centered in different triads: F_{AAA} , F_{AAB} and F_{BAB} for A-centered triads, for instance $F_w(A_1) \equiv F_{BAB}$. The calculated distribution functions are plotted in Figs. 1-6.

The influence of the copolymerization process on the copolymer microstructure is generally more pronounced in the medium composition range, for short blocks of MAP units, since depropagation affects only MAP terminated macroradicals, and since penultimate effects are stronger for the same type of growing chains. With respect to the terminal unit model, penultimate effects modify the unit distribution to a much greater extent than depolymerization. For instance,

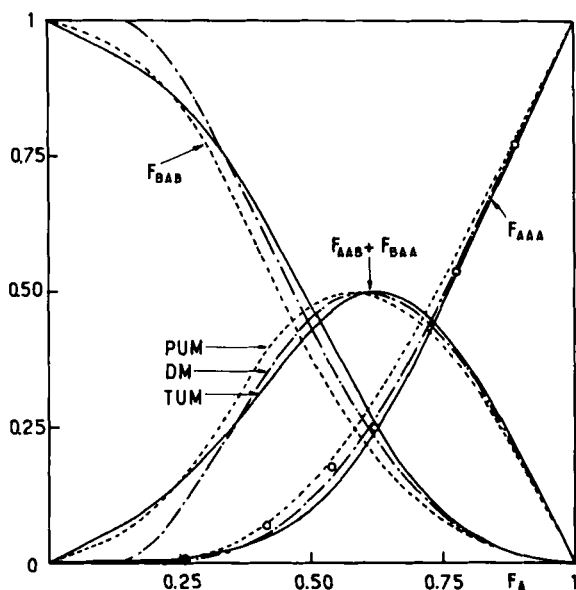


FIG. 1. Distribution of MMA A-centered triads vs. F_A molar fraction of MMA in the copolymer: (—) terminal unit model (TUM); (---) penultimate unit model (PUM); (- · -) depropagation model (DM); (○) NMR experimental points.

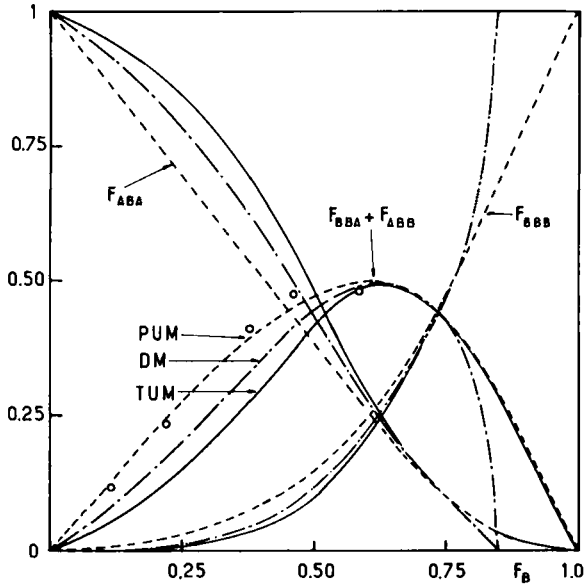


FIG. 2. Distribution of MAP B-centered triads vs. F_B , molar fraction of MAP in the copolymer. Same symbols as in Fig. 1.

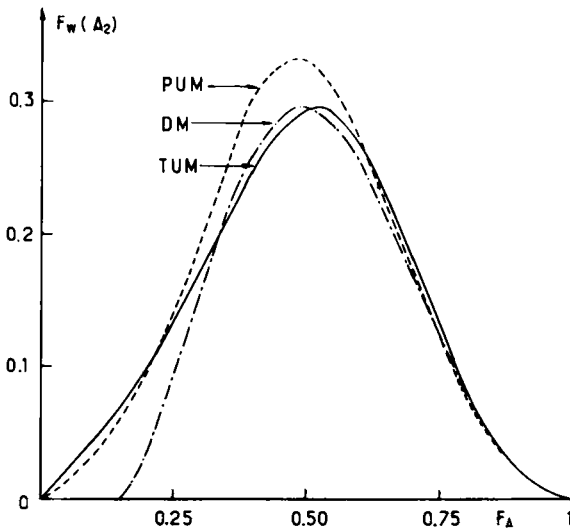


FIG. 3. Variations of the weight fraction of MMA units included in MMA dyads vs. F_A . Same symbols as in Fig. 1.

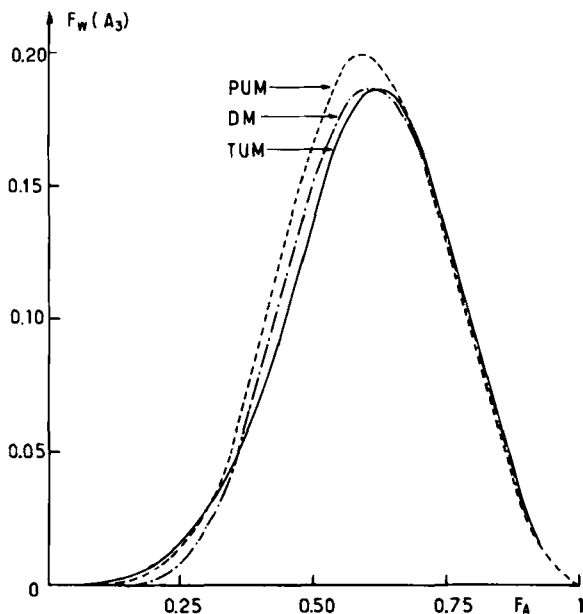


FIG. 4. Variations of the weight fraction of MMA units included in MMA triads vs. F_A . Same symbols as in Fig. 1.

for a copolymer including 35% MAP units, the fraction of isolated MAP units increases from 0.570 for the terminal unit model, to 0.660 for copolymerization with depropagation, and to 0.730 for the penultimate unit model; the fraction of MAP units included in MAP diads increases in the same order from 0.210 to 0.245 and to 0.425.

Such high differences clearly point out the major importance of a good choice of the copolymerization model, since the copolymer properties are mainly determined by microstructure: this can be easily imagined for the photochemistry of these ketonic copolymers, where energy transfer processes depend strongly on the distribution of the chromophoric units along the chain [10].

Analysis of Sequence Distribution in MMA-MAP Copolymers through $^1\text{H-NMR}$ Spectroscopy

$^1\text{H-NMR}$ spectroscopy on MMA-MAP copolymers in CDCl_3 solution at 60°C does not allow a rigorous analysis of sequence distribution,

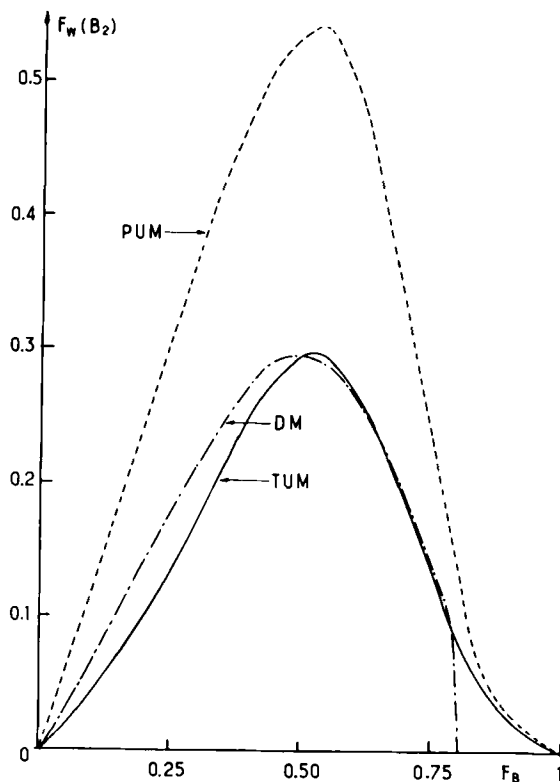


FIG. 5. Variations of the weight fraction of MAP units included in MAP dyads vs. F_B . Same symbols as in Fig. 1.

even if carried out at high field (220 and 250 MHz). The α -CH₃ resonance appears as a very broad, insufficiently resolved multiplet, and the -O-CH₃ methoxy resonance (singlet at 3.62 ppm) is not split according to compositional effects. On the other hand, the ¹H-NMR spectrum of the PMAP homopolymer is not resolved at 100 MHz [2] and only poorly resolved at 220 or 300 MHz [11]. The ¹H-NMR spectrum of our anionic PMAP sample, obtained at 250 MHz in CDCl₃ solution at 30° C, is given in Fig. 7.

The assignment of the resonance peaks and a rough estimation of tacticity according to Merle-Aubry [11] ($I = 2H_A/\text{total-CH}_2$) lead to values of $I = 0.57$, $S = 0.43$, in terms of dyads. It is possible that a

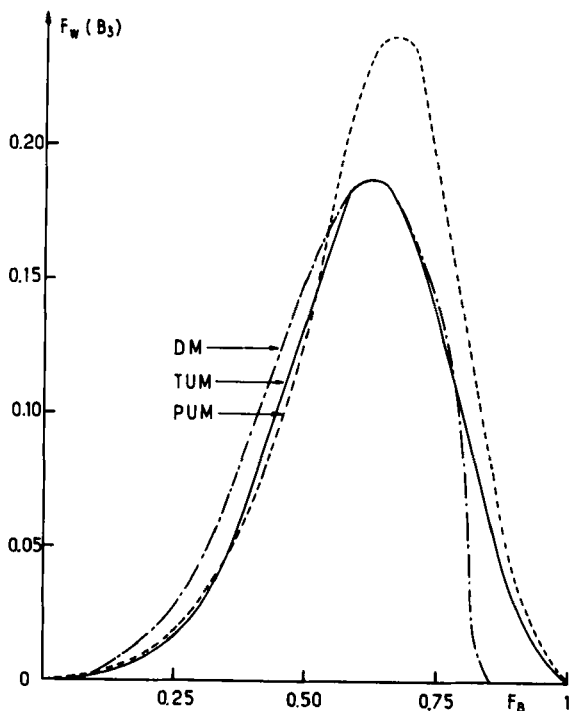


FIG. 6. Variations of the weight fractions of MAP units included in MAP triads versus F_B . Same symbols as in Fig. 1.

better choice of the experimental conditions, high temperature and aromatic solvents, for instance (the ^1H -NMR spectrum of PMMA at 220 MHz in chlorobenzene solution at 120°C is very well resolved [12]), would lead to sufficient improvement for the MMA-MAP copolymers; nevertheless, we have preferred to turn to ^{13}C - $[^1\text{H}]$ NMR spectroscopy.

Analysis of Sequence Distribution in MMA-MAP Copolymers through ^{13}C - $[^1\text{H}]$ NMR Spectroscopy

^{13}C - $[^1\text{H}]$ NMR Spectra of the Parent Homopolymers

The ^{13}C - $[^1\text{H}]$ NMR spectrum of PMMA is already well known [13-15], and Merle-Aubry [11] has recently reported the determination

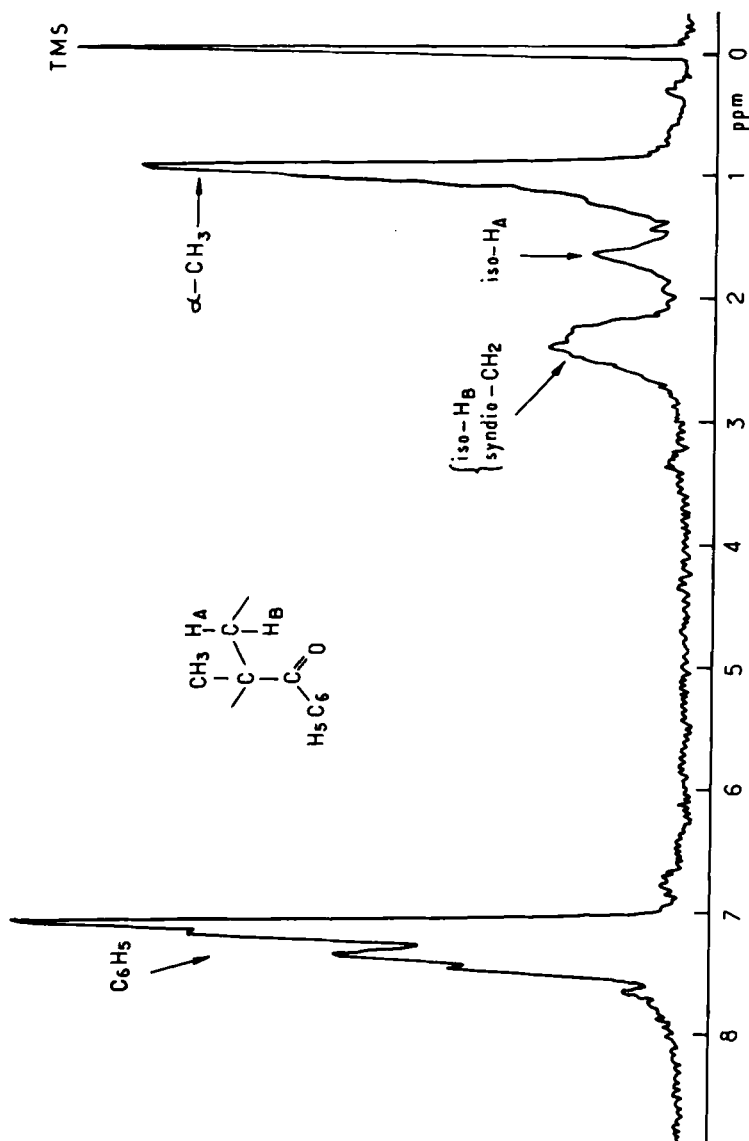


FIG. 7. ¹H-NMR spectrum of anionic PMAP obtained at 250 MHz (CDCl₃, 30°C).

of PMAP tacticity through ^{13}C - $[^1\text{H}]$ NMR spectroscopy. The spectrum in CDCl_3 solution at 30°C of our anionic PMAP sample is given in Fig. 8. The detailed analysis of this spectrum is out of the scope of this present communication, but an important feature has to be stressed. According to Merle-Aubry [11], the quaternary carbon atom is split into three main peaks according to triad tacticity: syndiotactic rr triads at 53.0 ppm, heterotactic mr triads at 52.8 ppm, isotactic mm triads at 52.5 ppm, the $\beta\text{-CH}_2$ resonance appearing as a poorly resolved multiplet at 54 ppm (the spectrum is not given in Merle-Aubry's thesis). On the other hand, we have confirmed that the resonance of the quaternary carbon atom of pivalophenone $(\text{CH}_3)_3\text{-C-CO-C}_6\text{H}_5$, chosen as a model compound for PMAP units, occurs at 44.18 ppm. Thus it seems more likely to ascribe to the quaternary carbon atom of PMAP the weak resonance observed at 36.57 ppm.

General Considerations on Application of ^{13}C - $[^1\text{H}]$ NMR Spectroscopy to Sequence Distribution Analysis in MMA-MAP Copolymers

The analysis of sequence distribution in copolymers by NMR spectroscopy is greatly simplified when the resonance splitting of a given nucleus belonging to one chemical unit only can be attributed exclusively to compositional sequence effects. For MMA-MAP copolymers we were not able to find NMR experimental conditions leading to such a convenient situation: for instance, the O-CH_3 methoxy resonance appears as a sharp singlet in PMMA ($\delta = 51.98$ ppm) and in MMA-MAP copolymers as well, independently of both tacticity and chemical environment. On the other hand, the $\alpha\text{-CH}_3$ carbon atoms of PMMA and PMAP, the quaternary carbon atom of PMMA, the carbonyl carbon atoms of the ester and keto functions already show great sensitivity to stereoregularity in the homopolymers; their complex patterns observed in the copolymers arise from simultaneous influence of compositional and configurational effects.

In the case of MMA-MAP copolymers, both MMA and MAP units may involve an asymmetric carbon atom. For a complete description of the copolymer microstructure it is necessary, for instance, to take into account as much as ten different triads with a central A unit which are actually NMR-distinguishable (Appendix II). Assuming that the configurational sequence distribution may be described by the conventional tacticity and cotacticity parameters σ_{AA} , σ_{AB} , σ_{BA} , and σ_{BB} as defined by Coleman [16] and Bovey [17], where σ_{ij} is the probability of generating a meso dyad between an i -terminated growing chain

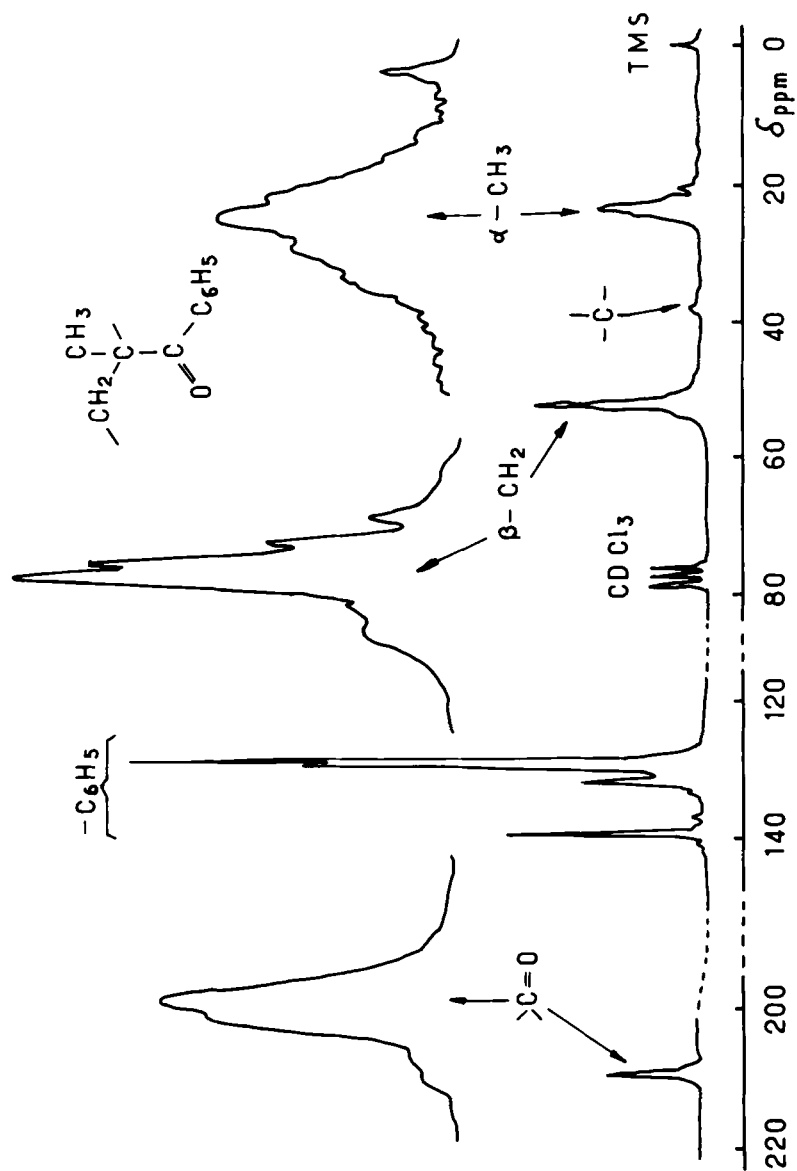


FIG. 8. ^{13}C [^1H]-NMR spectrum of anionic PMAP (CDCl_3 , 30°C).

and an incoming j monomer, one may obtain a set of equations correlating the fraction of A units centered in the different triads with the tacticity parameters [17]. The detailed calculations may be found in Appendix II.

The values of σ_{AA} for free-radical MMA polymerization are well known [18-20], $\sigma_{AA} \approx 0.243$ at 60°C , but the corresponding values of σ_{AB} and σ_{BA} are not accessible. Thus, for the three copolymerization models we have considered, it is not possible to perform a rigorous theoretical calculation of the fractions of the different A-centered triads by using the values of the reactivity ratios previously determined. In a first approach, on assuming that $\sigma_{AB} = \sigma_{BA} = \sigma$ [21], the various triads become function of a single unknown cotacticity parameter σ . Taking σ as an adjustable parameter ($0 \leq \sigma \leq 1$), one may compare the theoretical sequence distribution deduced from kinetic measurements (reactivity ratios) with the experimental distribution derived from NMR data, provided a correct assignment of the different resonance peaks may be found. Because of the lack of well defined model compounds, this assignment has been carried out by successive approximations, taking into account the variations of peak intensity with copolymer composition, and according to semi-empirical rules (perturbations in BAB triads with respect to the initial AAA triad are expected to be greater than in AAB triads, and so on). The final coherence test is that the proposed assignment has to lead to a single σ value for all the measured NMR peaks and for all the copolymers when NMR experimental and theoretical distributions of monomer units are correlated through the previously quoted equations (Appendix II). This may be considered as a rather drastic test, since a slight variation in the experimental determination of the various triad fractions may induce fairly higher changes in the calculated σ values. Such an approach has been used for various copolymers, and good illustrations may be found in the communication of Yamashita et al. [21] and in the references quoted therein.

We have focused our interest on the resolution of the quaternary carbon atom of PMMA units and of the $\alpha\text{-CH}_3$ carbon atom of MMA and MAP units.

Resonance Pattern of the Quaternary Carbon Atom of MMA Units

For all the investigated copolymers, the resonance area between 44.5 and 46 ppm is related to the quaternary carbon atom of MMA units (Fig. 9). In PMMA homopolymer, it is resolved into three well defined peaks centered at 45.74, 45.17, and 44.84 ppm for isotactic,

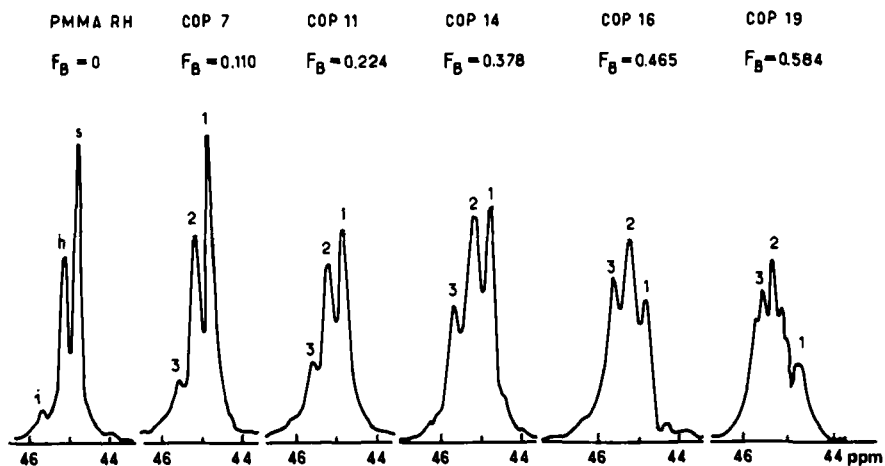


FIG. 9. ^{13}C - $[^1\text{H}]$ NMR spectra of MMA-MAP copolymers. Resonance patterns of the quaternary carbon atom of MMA units.

heterotactic, and syndiotactic triads, respectively, in good agreement with literature data [13-15]: $I = 0.056$, $H = 0.362$, $S = 0.582$ for the R-H free radical sample. As F_B , the molar fraction of MAP, increases up to 0.50 in the copolymers, these peaks undergo a characteristic broadening and change in relative intensity without any significant shift in frequency (45.63, 45.18 and 44.79 ppm). For $F_B = 0.58$, the resonance pattern is split into five peaks, and for $F_B = 0.75$ the complex multiplet is no better resolved.

We have checked that the splitting of this resonance does not arise from configurational effects alone, nor from compositional effects alone (all the triads of the same tacticity under the same resonance peak whatever their composition, or vice versa). The best assignment found for the three main peaks, their expression in function of the two tacticity parameters σ_{AA} and σ , and their experimental resonance area fraction are given in Table 1. With respect to PMMA homopolymer, these assignments may be rationalized in the following terms: replacement of one flanking A, either in meso or in racemic placement, by B with no change of the triad configuration does not alter the resonance frequency of the central A unit; replacement of the two flanking A by B shifts the resonance position downfield by about 0.42 ppm, provided at least one racemic placement is concerned.

TABLE 1. Analysis of the Resonance Pattern of the Quaternary Carbon Atom of MMA Units

Peak No.	δ (ppm)	Cotactic triads	Correlation with tacticity parameters ^a	NMR resonance area fraction for copolymers		
				Sample 7, $F_A = 0.890$	Sample 14, $F_A = 0.622$	Sample 19, $F_A = 0.416$
I	44.79	s(AAA)	$F_{AAA} \times (1 - \sigma_{AA})^2$	0.547	0.493	0.384
		s(AAB)	$F_{AAB} \times (1 - \sigma_{AA})(1 - \sigma)$	0.332	0.332	0.203
		h(AAA)	$F_{AAA} \times 2\sigma_{AA}(1 - \sigma_{AA})$			
II	45.18	h(AAB)	$F_{AAB} \times [\sigma_{AA}(1 - \sigma) + \sigma(1 - \sigma_{AA})]$	0.373	0.387	0.407
		s(BAB)	$F_{BAB} \times (1 - \sigma)^2$	0.409	0.409	0.443
		i(AAA)	$F_{AAA} \times \sigma_{AA}^2$			
III	45.63	i(AAB)	$F_{AAB} \times \sigma_{AA} \times \sigma$	0.080	0.120	0.208
		i(BAB)	$F_{BAB} \times \sigma^2$	0.258	0.258	0.354
		h(BAB)	$F_{BAB} \times 2\sigma(1 - \sigma)$			

^aWhen the resolution of these analytical expressions lead to two different σ values, only one is taken into account on the basis of its physical meaning.

Isotactic AAA and coisotactic BAB triads are not NMR-distinguishable.

The comparison between the calculated and the experimental values of the different triad fractions, through the set of equations of Table 1, allows the determination of the cotacticity parameter σ for every copolymer and for every resonance peak: the σ values thus obtained are collected in Table 2. Taking into account the accuracy of the measurements, chiefly for peak III which is the less important, the observed agreement between the calculated σ values for a given copolymerization process may appear reasonable. It confirms the peak assignment, and the assumption of a single value $\sigma_{AB} = \sigma_{BA} = \sigma$ which may be estimated to 0.37 ± 0.04 . On the other hand, the σ values deduced from peaks I and II are higher and less scattered for the different copolymers, assuming a penultimate unit model for copolymerization. Nevertheless, this better self-consistency cannot be considered as a direct proof in favor of this copolymerization process.

Resonance Pattern of the α -CH₃ Carbon Atoms of MMA and MAP Units

For all the investigated samples, the resonance area between 15.8 and 33 ppm is related to the α -CH₃ carbon atoms of both MMA and MAP units (Fig. 10). In PMMA homopolymer, it is resolved in three well defined peaks centered at 16.71, 18.90, and 21.51 ppm for isotactic, heterotactic, and syndiotactic triads respectively, in good agreement with literature data [13-15]: I = 0.053, H = 0.343, S = 0.604 for the R-H free-radical sample. In the anionic PMAP homopolymer, the α -CH₃ resonance pattern appears as a complex multiplet between 21 and 33 ppm; because of its poor resolution, it cannot be analyzed in term of tacticity [11]. For the MMA-MAP copolymers, the NMR spectrum, initially restricted to three main peaks obviously related to those of PMMA homopolymer for $F_B \leq 0.20$, becomes more and more complex as F_B increases. It would be fallacious to attempt a complete identification of the individual peaks among the twenty possible triads. We have taken into account only six main resonance areas we have been able to determine with sufficient accuracy, using the Du Pont 310 curve resolver. An illustration of such a simulation of these complex NMR patterns is given in Fig. 11 for copolymer 14 ($F_B = 0.378$). The best assignment found for these six contributions, their expression in function of the two tacticity parameters σ_{AA} and σ , and their experimental resonance area fraction are given in Table 3.

TABLE 2. σ Cotacticity Values Deduced from Analysis of the Resonance Pattern of the Quaternary Carbon Atom of MMA Units

Sample	F _A	σ Values											
		Terminal unit model			Depropagation model			Penultimate unit model					
		Peak I	Peak II	Peak III	Peak I	Peak II	Peak III	Peak I	Peak II	Peak III	Peak I	Peak II	Peak III
7	0.890	0.350	0.267	0.458	0.354	0.268	0.465	0.400	0.300	0.482			
11	0.776	0.375	0.287	0.429	0.381	0.290	0.437	0.397	0.330	0.459			
14	0.622	0.356	0.378	0.386	0.393	0.375	0.392	0.410	0.365	0.408			
16	0.523	0.392	0.370	0.386	0.400	0.369	0.392	0.420	0.355	0.370			
19	0.416	0.315	0.315	0.318	0.323	0.314	0.316	0.429	0.305	0.349			
	$\bar{\sigma}$	0.363	0.323	0.395	0.370	0.323	0.400	0.411	0.337	0.414			
	\pm	0.015	± 0.022	± 0.024	± 0.014	± 0.021	± 0.025	± 0.006	± 0.010	± 0.025			

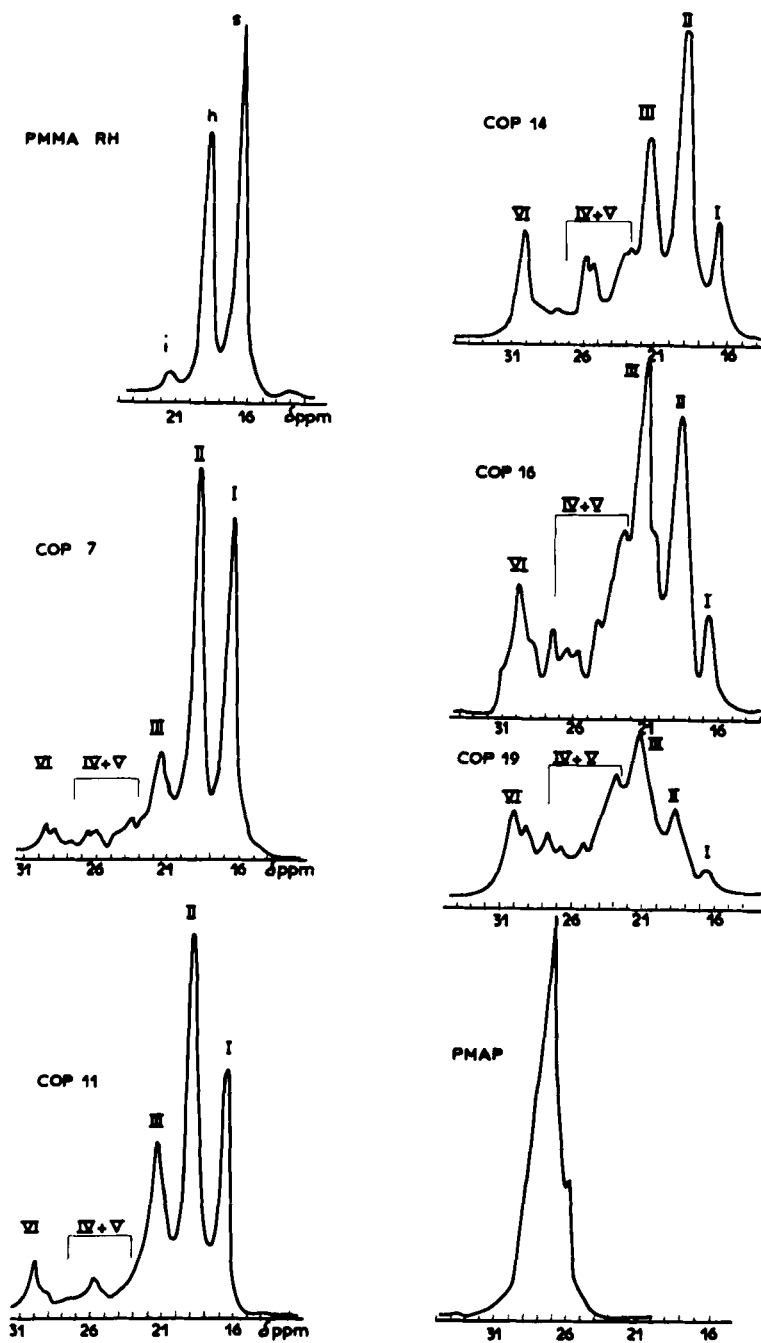


FIG. 10. ^{13}C - ^1H NMR spectra of MMA-MAP copolymers. Resonance patterns of the α - CH_3 carbon atom of MMA and MAP units.

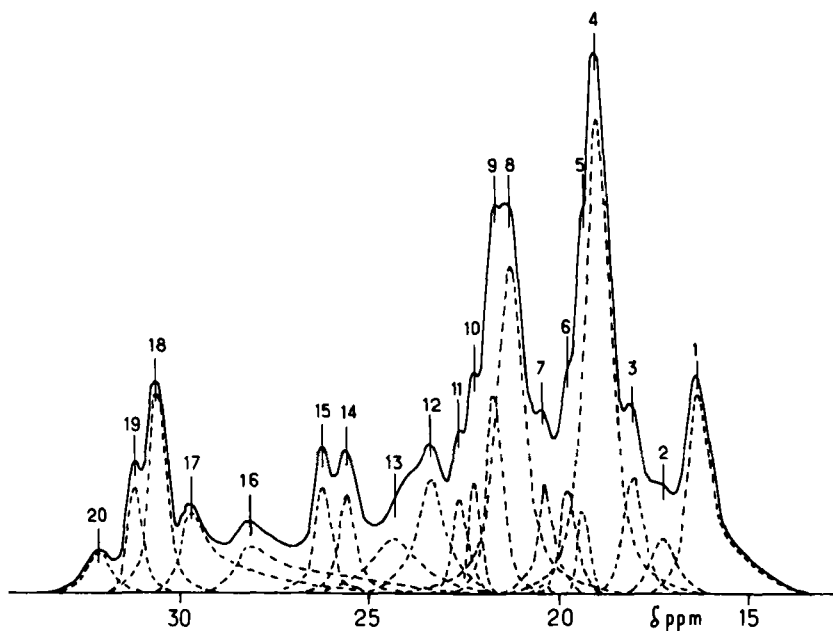


FIG. 11. ^{13}C - $[^1\text{H}]$ NMR spectrum of MMA-MAP copolymer 14 ($F_B = 0.378$). Simulation of the $\alpha\text{-CH}_3$ resonance pattern: (area I) peak 1; (area II) peaks 2-6; (area III) peaks 7-10; (area IV + V) peaks 11-16; (area VI) peaks 17-20.

With respect to the parent homopolymers, these assignments may be described in the following terms. For A-centered triads, replacement of one flanking A by B shifts the resonance frequency of the central A unit downfield only in the case of cosyndiotactic triads. This shift, however, occurs to a much greater extent when the two flanking A are replaced by B, whatever the configuration of the triad is. For B-centered triads, replacement of one, then two flanking B by A shifts the resonance frequency of the central B unit downfield and upfield, respectively, whatever the triad configuration is.

The triad fractions related to peaks I ($S(\text{AAA})$), I + II + III ($F_{\text{AAA}} + F_{\text{AAB}} + F_{\text{ABA}}$), IV + V ($F_{\text{BAB}} + F_{\text{BBB}}$) and VI (F_{BBA}) are independent of the cotacticity parameter σ , and their analysis thus allows a direct comparison between experimental and calculated distributions for the three copolymerization models without any assumption on the stereoregularity of the cross-propagation step.

TABLE 3. Analysis of the Resonance Pattern of the α -CH₃ Carbon Atom

Peak	δ (ppm)	Cotactic triads	Correlation with tacticity parameters ^a	NMR resonance area fraction for copolymers					
				Sample 7, F _A = 0.890	Sample 11, F _A = 0.776	Sample 14, F _A = 0.622	Sample 16, F _A = 0.535	Sample 19, F _A = 0.416	Sample
I	16.55	s(AAA)	$F_A \times F_{AAA}(1 - \sigma_{AA})^2$	0.395	0.246	0.092	0.062	0.012	
		h(AAA)	$F_A \times F_{AAA} \times 2\sigma_{AA}(1 - \sigma_{AA})$						
		h(AAB)	$F_A \times F_{AAB}[\sigma_{AA}(1 - \sigma) + \sigma(1 - \sigma_{AA})]$	0.418	0.422	0.343	0.280	0.153	
II	19.30- 19.8	s(AAB)	$F_A \times F_{AAB} \times (1 - \sigma_{AA})(1 - \sigma)$						
		i(AAA)	$F_A \times F_{AAA} \times \sigma_{AA}^2$						
III	21.4- 21.6	i(AAB)	$F_A \times F_{AAB} \times \sigma_{AA} \sigma$	0.161	0.221	0.244	0.245	0.192	
		ABA	$F_B \times F_{ABA}$						
IV + V	22.9- 25.0	BAB	$F_A \times F_{BAB}$	0.013	0.059	0.168	0.213	0.365	
		BBB	$F_B \times F_{BBB}$						
VI	30.5	BBA	$F_B \times F_{BBA}$	0.013	0.052	0.153	0.200	0.278	

^aSee Table 1 footnote.

The experimental points related to peak I [$s(\text{AAA})$] agree fairly well with the calculated curves (Fig. 1) but they do not allow a definite choice among the three copolymerization processes, even if the penultimate model seems to be preferred for high F_B values. This good agreement justifies the assumption that the stereochemistry of MMA homopropagation is not affected by MAP and still obeys Bernoulli statistics characterized by the value $\sigma_{AA} = 0.243$.

F_{BAB} and F_{BBB} triad fractions are separately sensitive to the copolymerization process, but their cumulative weight, measured by the poorly resolved resonance peaks IV + V, no longer shows such a dependence. The good agreement between experimental points and the calculated curve may be considered as a proof of a correct assignment of the resonance peaks, the penultimate unit model being slightly favored (Fig. 12). Quite the same situation occurs with the triad

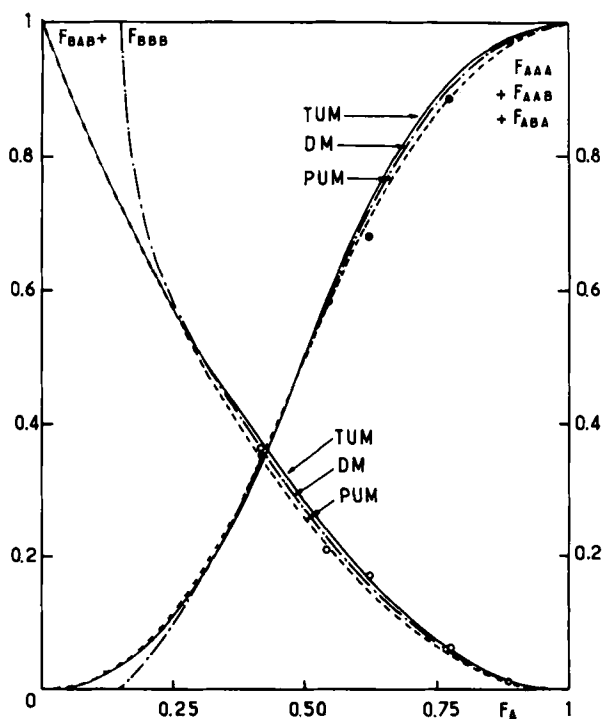


FIG. 12. Variation of (\circ) $F_{BAB} + F_{BBB}$ and (\bullet) $F_{AAA} + F_{AAB} + F_{ABA}$ triad fractions vs. F_A . Same symbols as in Fig. 1.

fractions $F_{AAA} + F_{AAB} + F_{ABA}$ related to peaks I + II + III, as shown in Fig. 12. The experimental points related to the F_{BBA} triad clearly fit the calculated curve assuming copolymerization with penultimate effects, and thus this model has to be preferred (Fig. 2).

On the other hand, the analysis of the resonance peaks II and III [$h(AAA) + h(AAB) + s(AAB)$ and $i(AAA) + i(AAB) + ABA$, respectively] allows determination of the cotacticity parameter σ as previously described. The calculated σ values for all the copolymers and for the three copolymerization models are collected in Table 4.

The terminal unit and the depropagation models lead to strongly scattered σ values, and even to a meaningless negative one for a given peak on a given copolymer in some cases. On the contrary, the penultimate unit model gives a well defined σ value, $\sigma = 0.41 \pm 0.01$. Moreover, this value is in fair agreement with the previous one 0.37 ± 0.04 resulting from the analysis of the resonance pattern of the quaternary carbon atom of MMA units assuming the same copolymerization model. All these features are strong arguments in favor of the penultimate effects.

Stereochemistry of the Cross Propagation in MMA-MAP Free-Radical Copolymerization at 60°C

The stereochemistry of the cross propagation in free-radical copolymerization of 1,1-disubstituted ethylenic monomers with MMA at 60°C obviously depends on the comonomer structure. Syndiotactic placements are highly favored for α -methylstyrene-MMA ($\sigma = 0.27$ [9, 21]) and for methacrylic acid-MMA ($\sigma = 0.20$ [22]), as for MMA homopolymerization ($\sigma_{AA} = 0.24$); they are much less favored for tritylmethacrylate-MMA ($\sigma = 0.41$ [23]). The MMA-MAP system seems quite similar to the latter case, and its high σ value ($\sigma = 0.40$) shows that cross propagation is not very different from a pure atactic process ($\sigma = 0.50$).

The stereostructure of free radical methacrylic ester polymers may depend on both steric and polarity factors [24, 25]: bulkiness, rigidity, and polarizability of the ester group, or more specific interactions between the ester groups. It is generally observed that an increase of these parameters favors the formation of isotactic helical segments [26-28].

In the previous communication [1] we have shown that the phenyl ring $\pi - \pi^*$ UV transition of the aromatic keto chromophore is the same for anionic PMAP homopolymer and for free radical MMA-MAP copolymers: identical line shapes, and identical molar absorptivity $\epsilon = 7830$ liter/mole-cm at $\lambda = 243$ nm in dioxane solution. This

TABLE 4. σ Cotacticity Values Deduced from Analysis of the Resonance Pattern of the α -CH₃ Carbon Atom

Sample	FA	σ Values					
		Terminal unit model		Depropagation model		Penultimate unit model	
		Peak II	Peak III	Peak II	Peak III	Peak II	Peak III
7	0.890	0.519	0.426	0.469	0.454	0.415	0.390
11	0.776	0.490	0.070	0.437	0.223	0.429	0.408
14	0.622	0.476	-0.221	0.386	-0.008	0.419	0.397
16	0.523	0.665	0.019	0.555	0.067	0.397	0.419
19	0.416	-0.039	-0.028	-0.156	0.468	0.407	0.420
	$\bar{\sigma}$	0.422	0.053	0.338	0.240	0.413	0.407
		± 0.125	± 0.105	± 0.127	± 0.097	± 0.005	± 0.006

independence of unit distribution seems to rule out strong specific interactions between ester and aromatic keto functions, which would require a definite geometry of placement of monomeric units in an AB dyad. This feature, however, has not to be taken as definitely conclusive, since UV transitions in random copolymers may be affected by the solvent polarity [29]. On the other hand, examination of copolymer architecture, simulated by an AABA tetrad for instance, on Corey-Pauling-Koltun or Courtauld atomic models clearly shows that the great steric hindrance of the aromatic keto function leads to a high rigidity and a very compact structure of the polymeric chain, but it does not allow a preferential choice between meso and racemic placements in an AB dyad on the basis of steric requirements alone. Thus, the high σ value calculated for the MMA-MAP cross propagation may be tentatively attributed to the great steric hindrance and the high polarizability of the aromatic keto group.

CONCLUSION

All the kinetic results related to the MMA-MAP free radical copolymerization at 60 °C [1] and all the structural data related to the copolymers may be readily taken into account within the following scheme. Copolymerization obeys a penultimate unit model characterized by the four reactivity ratios: $r_{AA} = 1.77 \pm 0.02$, $r_{BA} = 2.30 \pm 0.10$, $r_{BB} = 0.058 \pm 0.01$, $r_{AB} = 0.325 \pm 0.03$. The propagation stereochemistry obeys Bernoulli statistics, characterized by the tacticity parameters: $\sigma_{AA} = 0.243$ and $\sigma_{AB} = \sigma_{BA} = 0.40$.

This copolymerization scheme has to be considered merely as a convenient model, because of some underlying approximations. MMA free-radical polymerization at 60 °C is not strictly Bernoullian [30], and the assumption that the stereochemistry of cross propagation is described by a single cotacticity parameter may be oversimplified. We have already pointed out that MMA-MAP copolymerization mainly depends on steric effects [1]. It is not quite satisfactory to describe the propagation steps according to a second-order Markov process for kinetics, taking into account the chemical structure of the terminal dyads of the growing chains, and according to simple Bernoulli statistics for the stereochemistry of the same process. Nevertheless, the proposed copolymerization model may be considered quite self-consistent and reasonably well justified by the several independent checks of the analysis of the experimental results. Penultimate effects are thought to rest on a rigorous physical ground from the

identification and the estimation of F_{BBA} triads, without any assumption on the stereochemistry of the copolymerization process.

Our study does not allow to clarify the origin of the penultimate effects. Owing to the great steric hindrance of MAP, it may be found in depolymerization of $\sim\sim AB\cdot$ and $\sim\sim BB\cdot$ growing chains, not necessarily according to Lowry's schemes. In this sense, it would be interesting to study in a wide range the influence of temperature and concentration on the copolymerization process (concentration has practically no influence between 4.4 and 8.8 mole/liter [1]), but this is far beyond the scope of the present work.

We hope that the proposed copolymerization model will prove its interest and find further justification in the study of the correlations between copolymer photodegradation properties and copolymer microstructure [31].

APPENDIX I: SEQUENCE DISTRIBUTION IN COPOLYMERS

Terminal Unit and Penultimate Unit Models

In these two cases, the statistics of sequence distribution in copolymers has received much attention, and a complete description of copolymer composition and microstructure may be found in the paper of Ito and Yamashita [32] and in the references quoted therein. The most important relationships are collected in Table 5.

Copolymerization with Depropagation

Following the pioneering kinetic study of Lowry [33] on the effect of depropagation on copolymer composition, several authors have focused their interest on the problem of sequence distribution from probability considerations. Johnsen and Kolbe [8] and later O'Driscoll et al. [34] derived theoretical expressions which have been proved useful for comparison with experimental distribution as deduced from NMR measurements, when depropagation occurs through dyad end groups [8, 9] (Lowry's case I). We have previously shown [1] that MMA-MAP copolymerization may be affected by depropagation of MAP according to Lowry's case II, where depropagation takes place only for B triad end groups:

TABLE 5. Sequence Distribution in Copolymers^a

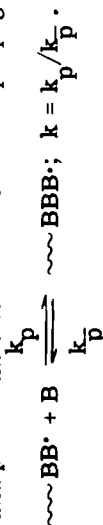
Terminal unit model	Penultimate unit model	Depropagation model
$P_{AA} = \frac{r_A(f_A/f_B)}{1 + r_A(f_A/f_B)}$	$P_{AAA} = \frac{r_{AA}(f_A/f_B)}{1 + r_{AA}(f_A/f_B)}$	$P_{AA} = \frac{r_A(f_A/f_B)}{1 + r_A(f_A/f_B)}$
$P_{AB} = \frac{1}{1 + r_A(f_A/f_B)}$	$P_{AAB} = \frac{1}{1 + r_{AA}(f_A/f_B)}$	$P_{AB} = \frac{1}{1 + r_A(f_A/f_B)}$
	$P_{BAA} = \frac{r_{BA}(f_A/f_B)}{1 + r_{BA}(f_A/f_B)}$	$P_{BA} = P_{AB} \frac{F_A}{F_B}$
	$P_{BAB} = \frac{1}{1 + r_{BA}(f_A/f_B)}$	$P_{BB} = 1 - P_{AB} \frac{F_A}{F_B}$
$F_{AAA} = P_{AA}^2$	$F_{AAA} = \frac{P_{BAA} + P_{AAA}}{P_{BAA} + P_{AAB}}$	
$F_{AAB} = 2 P_{AA} P_{AB}$	$F_{AAB} = \frac{2 P_{AAB} \cdot P_{BAA}}{P_{AAB} + P_{BAA}}$	

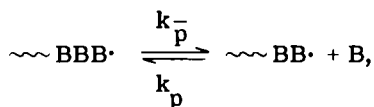
(continued)

TABLE 5 (continued)

Terminal unit model	Penultimate unit model	Depropagation model
$F_{BAB} = F_w(A_1) = P_{AB}^2$	$F_{BAB} = F_w(A_1) = \frac{P_{AAB} P_{BAB}}{P_{AAB} + P_{BAA}}$	
$\left. \begin{array}{l} F_w(A_n) = n P_{AB} P_{AA}^{n-1} \\ \text{with } n > 1 \end{array} \right\}$	$\left. \begin{array}{l} F_w(A_n) = \frac{n P_{AAB} P_{BAA} P_{AAA}^{n-2}}{P_{AAB} + P_{BAA}} \\ \text{with } n > 1 \end{array} \right\}$	

f_A and f_B are the molar fractions of monomer A and B in the monomer feed. F_A and F_B are the molar fractions of monomer A and B in the copolymer. A and B are symmetrical variables for terminal and penultimate unit model. The depropagation model is





with

$$k = k_p/k_p^-$$

The general theoretical expressions of sequence distribution are complex [34]. As suggested by O'Driscoll et al. [34], simple relationships may be readily obtained by taking into account the following assumptions: terminated $\sim\text{AA}\cdot$ macroradicals do not depropagate, and A sequence distribution may be calculated by using the terminal unit model; whatever the copolymerization process is, $P_{\text{BA}}/P_{\text{AB}} = F_{\text{A}}/F_{\text{B}}$ and $P_{\text{BA}} + P_{\text{BB}} = 1$. The conditional probabilities that a B-terminated macroradical will add an A or a B unit may thus be calculated from the homologous conditional probability P_{AB} and the copolymer composition. The depropagation effects are included in the compositional term $F_{\text{A}}/F_{\text{B}}$ through the equations developed by Lowry [33].

F_{A} and F_{B} are functions of the propagation-depropagation equilibrium constant [Eqs. (17), (18), (25), and (26) in Lowry's paper]. B sequence distribution is easily derived from the conditional probabilities P_{BB} and P_{BA} . The main relationships are summarized in Table 5.

NOTE: Equations (83) and (87) in the paper of O'Driscoll et al. [34] were given incorrectly in the original paper and they must be replaced by:

$$(\text{BB}) = [r_2 - (\eta \nu r_2)/\rho] / \{1 + r_1 + [1 + r_2 - (\eta \nu r_2)/\rho]\} \quad (83)$$

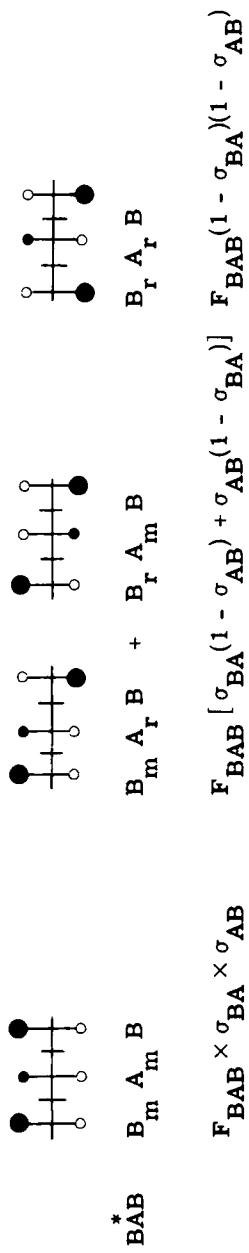
$$(\text{B}_n - \text{B}_{n-1}) = (\text{B}) - (\text{A}) \{1/[1 + r_1(\text{A})/(\text{B})]\} \quad (87)$$

APPENDIX II: COMPOSITIONAL AND CONFIGURATIONAL EFFECTS ON SEQUENCE DISTRIBUTION IN MMA-MAP COPOLYMERS

A comprehensive description of configurational sequences in copolymers may be found in the reviews of Bovey [35] and of Klesper

TABLE 6. Configurational Sequence Distribution for MMA-MAP Copolymers According to Bernoulli Statistics

Triads	Coisotactic triads	Coheterotactic triads	Cosyndiotactic triads
* AAA			
	$A_m A_m A$	$A_m A_r A + A_r A_m A$	$A_r A_r A$
	$F_{AAA} \times \sigma_{AA}^2$	$F_{AAA} \times 2 \sigma_{AA} (1 - \sigma_{AA})$	$F_{AAA} (1 - \sigma_{AA})^2$
* AAB			
+ BAA			
	$A_m A_m B + B_m A_m A$	$A_m A_r B + B_r A_m A$	$A_r A_r B + B_r A_r A$
	$F_{AAB} \times \sigma_{AA} (\sigma_{AB} + \sigma_{BA})$	$F_{AAB} \times \sigma_{AA} [(1 - \sigma_{AB}) + (1 - \sigma_{AA})]$	$F_{AAB} \times (1 - \sigma_{AA}) [(1 - \sigma_{AB}) + (1 - \sigma_{BA})]$
	$A_r A_m B + B_m A_r A$	$A_r A_m B + B_m A_r A$	
	$F_{AAB} \times (1 - \sigma_{AA}) (\sigma_{AB} + \sigma_{BA})$		



^aSymbols: O, α -CH₃; ●, -CO₂-CH₃, ●, -CO-C₆H₅, ---, β -CH₂.

and Sielaff [36]. In MMA-MAP copolymers, each of the comonomers may form an asymmetric C atom: because of the simultaneous compositional and configurational effects, the complete analysis of the copolymer microstructure requires to take into account ten different A- (or B-) centered triads which are actually NMR distinguishable. Assuming that the configurational sequence distribution may be described by Bernoulli statistics, one can obtain a set of equations correlating the fraction of A (or B) units centered in the different triads with the conventional tacticity parameters σ_{AA} , σ_{AB} , σ_{BB} and σ_{BA} [17]. The detailed illustration of such an analysis is given in Table 6 for A-centered triads (A and B are obviously symmetrical variables).

ACKNOWLEDGEMENTS

The NMR spectra were run by Mr. Maltese (L. Pasteur University of Strasbourg), and their simulation on a Du Pont 310 curve resolve was made possible through the kindness of Dr. Pham Quang Tho.

We are greatly indebted to Prof. Weill and Dr. Rempp for helpful discussions and a critical survey of the manuscript.

REFERENCES

- [1] R. Roussel, M. Galin, and J. C. Galin, J. Macromol. Sci.-Chem., **A10**, 1479 (1976).
- [2] J. E. Mulvaney, J. G. Dillon, and J. L. Laverty, J. Polym. Sci. A-1, **6**, 1841 (1968).
- [3] J. Schaefer, Macromolecules, **4**, 98 (1971).
- [4] M. Berger and I. Kuntz, J. Polym. Sci. A, **2**, 1687 (1964).
- [5] K. H. Hellwege, U. Johnsen, and K. Kolbe, Kolloid Z., **214**, 45 (1966).
- [6] J. B. Kinsinger, T. Fischer, and C. W. Wilson III, J. Polym. Sci. B, **4**, 379 (1966); Ibid., **5**, 285 (1967).
- [7] J. Guillet, A. Guyot, and Q. T. Pham, J. Macromol. Sci.-Chem., **A2**, 1303 (1968).
- [8] U. Johnson and K. Kolbe, Makromol. Chem., **116**, 173 (1968).
- [9] M. Izu, K. F. O'Driscoll, R. J. Hill, M. J. Quinn, and H. J. Harwood, Macromolecules, **5**, 90 (1972).
- [10] J. E. Guillet, in Degradation and Stabilization of Polymers, G. Geuskens, Ed., Applied Science Publishers, London, 1975, p. 181.

- [11] L. Merle-Aubry, Thesis, University of Rouen, 1975.
- [12] R. C. Ferguson, Macromolecules, **2**, 237 (1969).
- [13] L. F. Johnson, F. Heatley, and F. A. Bovey, Macromolecules, **3**, 175 (1970).
- [14] Y. Inoue, A. Nishioka and R. Chujo, Polym. J., **2**, 535 (1971).
- [15] I. R. Peat and W. F. Reynolds, Tetrahedron Letters, 1972, 1359.
- [16] B. Coleman, J. Polym. Sci., **31**, 155 (1958).
- [17] F. A. Bovey, J. Polym. Sci., **62**, 197 (1962).
- [18] F. A. Bovey, J. Polym. Sci., **46**, 59 (1960).
- [19] T. G. Fox and H. W. Schnecko, Polymer, **3**, 575 (1963).
- [20] T. Otsu, B. Yamada, and M. Imoto, J. Macromol. Sci., **1**, 61 (1966).
- [21] K. Ito, S. Iwase, K. Umehara, and Y. Yamashita, J. Macromol. Sci.-Chem. **A1**, 891 (1967).
- [22] E. Klesper and W. Gronski, J. Polym. Sci. B, **7**, 727 (1969).
- [23] A. Yamada and J. Tanaka, paper presented at 23rd Symposium on Macromolecular Science, Tokyo, 1974.
- [24] D. J. Cram and H. R. Kopecky, J. Amer. Chem. Soc., **81**, 2748 (1959).
- [25] C. E. H. Bawn and A. Ledwith, Quart. Rev., **16**, 361 (1964).
- [26] T. Tsuruta, T. Makimoto, and H. Kanai, J. Macromol. Sci., **1**, 31 (1966).
- [27] J. Niezette and V. Desreux, Makromol. Chem., **149**, 177 (1971).
- [28] K. Matsuzaki, T. Kanai, K. Yamawaki, and K. P. Samre Rung, Makromol. Chem., **174**, 215 (1973).
- [29] B. M. Gallo and S. Russo, J. Macromol. Sci.-Chem., **A8**, 521 (1974).
- [30] M. Reinmüller and T. G. Fox, paper presented at American Chemical Society Meeting, 1966; Polym. Preprints, **7**, 999 (1966).
- [31] J. Guillet, unpublished results.
- [32] K. Ito and Y. Yamashita, J. Polym. Sci. A, **3**, 2165 (1965).
- [33] G. G. Lowry, J. Polym. Sci., **42**, 463 (1960).
- [34] J. A. Howell, M. Itsu and K. F. O'Driscoll, J. Polym. Sci. A-1, **8**, 699 (1970).
- [35] F. A. Bovey, in High Resolution NMR of Macromolecules, Academic Press, New York, 1972, p. 205.
- [36] E. Klesper and G. Sielaff, in Polymer Spectroscopy, D. O. Hummel, Ed., Verlag Chemie, Weinheim, 1974, p. 189.

Accepted by editor May 20, 1976

Received for publication July 22, 1976